

Low thermal conductivity of CsBiNb₂O₇ epitaxial layers

David G. Cahill, Alexander Melville, Darrell G. Schlom, and Mark A. Zurbuchen

Citation: *Applied Physics Letters* **96**, 121903 (2010); doi: 10.1063/1.3368120

View online: <http://dx.doi.org/10.1063/1.3368120>

View Table of Contents: <http://scitation.aip.org/content/aip/journal/apl/96/12?ver=pdfcov>

Published by the AIP Publishing

Articles you may be interested in

[Thermal conductivity changes upon neutron transmutation of 10B doped diamond](#)

J. Appl. Phys. **116**, 083706 (2014); 10.1063/1.4892888

[Thermal conductivity of nano-grained SrTiO₃ thin films](#)

Appl. Phys. Lett. **101**, 231908 (2012); 10.1063/1.4769448

[Thermal conductivity and photoluminescence of light-emitting silicon nitride films](#)

Appl. Phys. Lett. **100**, 051908 (2012); 10.1063/1.3682508

[Analysis of thermoreflectance signals and characterization of thermal conductivity of metal thin films](#)

Rev. Sci. Instrum. **80**, 124901 (2009); 10.1063/1.3265994

[Lower limit to the lattice thermal conductivity of nanostructured Bi₂Te₃-based materials](#)

J. Appl. Phys. **106**, 073503 (2009); 10.1063/1.3226884

The advertisement features a dark blue background with three images: a mobile phone, a desktop computer, and an AFM. Text on the left asks 'You don't still use this cell phone or this computer' and 'Why are you still using an AFM designed in the 80's?'. Text on the right promotes an upgrade with a '\$20,000 trade-in discount' and identifies 'Asylum Research' as the 'today's technology leader in AFM'. The Oxford Instruments logo and tagline 'The Business of Science' are at the bottom right, along with the email 'dropmyoldAFM@oxinst.com'.

Low thermal conductivity of CsBiNb₂O₇ epitaxial layers

David G. Cahill,^{1,a)} Alexander Melville,² Darrell G. Schlom,² and Mark A. Zurbuchen³

¹Department of Materials Science and Engineering, Materials Research Laboratory, University of Illinois, Urbana, Illinois 61801, USA

²Department of Materials Science and Engineering, Cornell University, Ithaca, New York, 14853, USA

³Department of Microelectronics Technology, The Aerospace Corporation, El Segundo, California 90245, USA

(Received 31 January 2010; accepted 26 February 2010; published online 23 March 2010)

The thermal conductivity of an epitaxial layer of CsBiNb₂O₇ grown by pulsed-laser deposition is measured by time-domain thermoreflectance in the temperature range 100 < *T* < 600 K. Characterization by x-ray diffraction and cross-sectional transmission electron microscopy show that the sample has the *n*=2 structure of the Dion–Jacobson series of phases. The conductivity of this layered oxide is ≈60% of the predicted minimum thermal conductivity in this temperature range; the thermal conductivity at room temperature, 0.4 W m⁻¹ K⁻¹, is comparable to the lowest conductivity ever observed in an oxide crystal. © 2010 American Institute of Physics.

[doi:10.1063/1.3368120]

Ultralow thermal conductivities—conductivities lower than predicted by the model of the minimum thermal conductivity¹—have been observed in layered thin film materials.^{2,3} The structures of the ultralow conductivity materials studied to-date, are not, however, equilibrium phases and therefore these materials are not stable at elevated temperatures where low thermal conductivity materials might find applications as thermal barriers. In this work, we have identified extremely low thermal conductivities in an equilibrium oxide crystal structure, the *n*=2 Dion–Jacobson phase of CsBiNb₂O₇. The conductivity at room temperature, ≈0.4 W m⁻¹ K⁻¹, is a factor of ≈5 less than the thermal conductivity of the most commonly used thermal barrier, yttria-stabilized zirconia.

A recent computational study⁴ found a minimum in the cross-plane thermal conductivity for the *n*=4 member of the Ruddelsden–Popper series of phases Sr_{*n*+1}Ti_{*n*}O_{3*n*+1}. The structure can be described as the periodic stacking along the *c*-axis of *n*SrTiO₃ perovskites layers and one SrO rocksalt layer; the repeat distance between SrO rocksalt layers along the *c*-axis of the *n*=4 member is ≈2 nm. CsBiNb₂O₇ has similar structural features: CsBiNb₂O₇ forms in the *n*=2 member of the Dion–Jacobson homologous series of phases, A[A'_{*n*-1}B_{*n*}O_{3*n*+1}], and can be described by NbO₆⁵⁻ octahedra interleaved between alternating BiO and Cs layers along its *c*-axis. The space group is P2₁*am* at room temperature.⁵ (Unstable phonons of the P4/*mmm* prototype drive the transition to P2₁*am*.⁶) The repeat distance between Cs layers along the *c*-axis^{5,7} is 1.14 nm.

To study cross-plane thermal transport, CsBiNb₂O₇ must be synthesized in epitaxial form; only polycrystalline synthesis has been reported previously.^{5,7}

Targets for pulsed-laser deposition (PLD) were synthesized by mixing powders of Bi₂O₃ (99.999% pure), Cs₂CO₃ (99.994% pure), and Nb₂O₅ (99.9985% pure) with a stoichiometric Cs:Bi:Nb atomic ratio of 1:1:2 and sintering in air at 900 °C for 150 min. Films were synthesized by PLD from this single target using a KrF excimer laser, λ=248 nm, un-

der oxidizing conditions in a 100 mTorr O₂/O₃ atmosphere (≈8% O₃), at 650 °C using a radiatively heated substrate holder⁸ and (110)-oriented NdGaO₃ single crystal substrates. Films were quenched immediately after growth to avoid decomposition by bismuth suboxide or cesium suboxide volatilization. Characterization by x-ray diffraction (XRD) was performed using four-circle x-ray diffractometry and Cu Kα radiation with a graphite incident-beam monochromator.

Cross-sectional samples for transmission electron microscopy (TEM) were prepared by focused ion beam milling. Samples were examined in a field-emission instrument at 300 keV by standard and scanning TEM (STEM) with a high-angle annular dark-field detector.

The as-grown films of CsBiNb₂O₇/(110) NdGaO₃ are *c*-axis oriented and nearly phase pure, as shown by the $\theta-2\theta$ and ϕ XRD scans in Figs. 1(a) and 1(b). The full-width at half-maximum of the rocking curve ω -scan of the 005 peak (not shown), and the ϕ -scan of the 111 peak in Fig. 1(b), are 0.32° and 1.05°, respectively. Two small impurity peaks appear in the $\theta-2\theta$ scan at 12.9° and 34.5°, and are believed to correspond to either Bi₂O₃ or Cs₂O impurity phases. Note that the intensities of these impurity peaks are two orders of magnitude lower than the major film peaks. This, together with the TEM and XRD analysis described below indicates that the film is an *n*=2 Dion–Jacobson phase. The *c*-axis lattice parameter, calculated by Nelson–Riley analysis,⁹ is 1.133 ± 0.001 nm.

TEM characterization is necessary for confirmation of large-period superlattice phases such as this, which are difficult to discern from intergrowths of multiple shorter-period members by XRD alone.^{10,11} The region imaged by STEM was taken from the same spot on the same film used for thermal conductivity measurements, and allowed precise measurement of the thickness needed for analyzing the data obtained in the time-domain thermoreflectance (TDTR) measurements of the thermal conductivity. A cross-sectional STEM image is shown in Fig. 2, with the substrate situated at the bottom. The film-substrate interface is sharp, and the film is free from intergrowths of Dion–Jacobson phases with other values of *n*, but we note the existence of some stacking faults and defective regions. We observed local variations of

^{a)}Electronic mail: d-cahill@uiuc.edu.

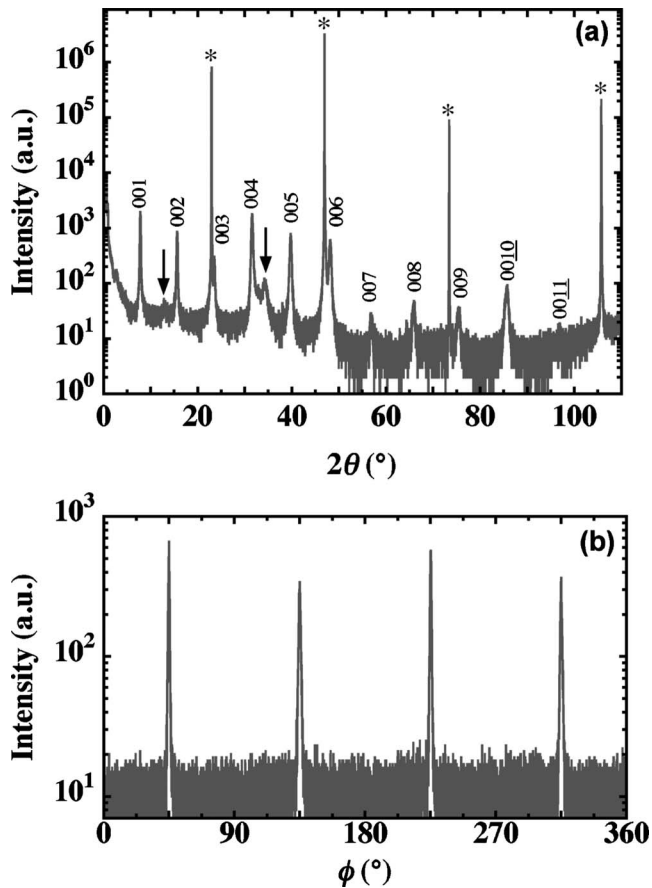


FIG. 1. Characterization of the $\text{CsBiNb}_2\text{O}_7$ film by XRD. (a) θ - 2θ scan and (b) ϕ scan of the 111 peak of $\text{CsBiNb}_2\text{O}_7$ indicate an epitaxial and nearly phase-pure film. Arrows indicate two small impurity peaks.

the total film thickness on the order of 10% in some regions, possibly caused by beads of decomposition products on the growth surface.

Our system for measurements of TDTR has been thoroughly validated and extensively applied in our studies of the thermal conductivity of thin films,^{3,12} the thermal conductance of interfaces,¹³ and micron-scale mapping of the ther-

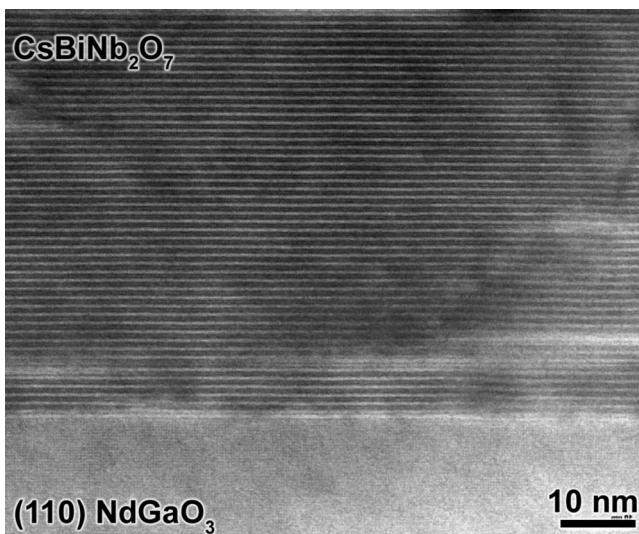


FIG. 2. Cross-sectional high-angle annular dark-field STEM image of the $\text{CsBiNb}_2\text{O}_7$ film, viewed along the [110] azimuth. A sharp film-substrate interface and some stacking faults are evident.

mal conductivity of bulk specimens.¹⁴ Techniques for analyzing TDTR data are described in Ref. 15; further details of the sensitivities and uncertainties of the measurements as a function of thermal conductivity, film thickness and modulation frequency are discussed in Ref. 12. Analysis of the TDTR data requires as an input the heat capacities per unit volume of the $\text{CsBiNb}_2\text{O}_7$ layers and NdGaO_3 substrate. Since we are not aware of any published data for the heat capacity of $\text{CsBiNb}_2\text{O}_7$, we used the heat capacity of $\text{Cd}_2\text{Nb}_2\text{O}_7$ to analyze the data;¹⁶ because the thickness of the $\text{CsBiNb}_2\text{O}_7$ layer is comparable to the thermal penetration depth d of the thermal waves used in the TDTR experiment, $d = \sqrt{D/(\pi f)}$ where D is the thermal diffusivity and $f = 9.8$ MHz is the modulation frequency of the pump beam, the sensitivity of the TDTR data to the heat capacity of the $\text{CsBiNb}_2\text{O}_7$ layer is much smaller than the sensitivity to the thermal conductivity¹² and any systematic errors introduced by uncertainties in the heat capacity are smaller than the other uncertainties in the experiment.

Most of the thermal resistance in the sample comes from the $\text{CsBiNb}_2\text{O}_7$ layer and therefore the data analysis is relatively insensitive to the thermal properties of the substrate. The thermal conductivity and heat capacity of the NdGaO_3 substrate were taken from Ref. 17. The authors of Ref. 17 measured the heat capacity of NdGaO_3 from 2.2 to 100 K but also plot previous data¹⁸ that extend to 300 K. Above 300 K, the heat capacities of NdGaO_3 and $\text{Cd}_2\text{Nb}_2\text{O}_7$ closely approach the classical Dulong-Petit limit; we extrapolate between the highest temperature data and the classical limit using the heat capacity of SrTiO_3 scaled by the relative Debye temperatures and atomic densities. We extrapolate the thermal conductivity of NdGaO_3 using a $1/T$ temperature dependence.¹⁷

Figure 3 summarizes the principal result of our work; the thermal conductivity for $\text{CsBiNb}_2\text{O}_7$ is extremely small for an oxide, only $\approx 0.4 \text{ W m}^{-1} \text{ K}^{-1}$ near room temperature. In fact, the conductivity is even smaller than the prediction of the model of the minimum thermal conductivity.¹ In the high temperature limit, $\Lambda_{\min} = 0.40 k_B n^{2/3} (v_l + 2v_t)$, where $n = 6.5 \times 10^{22} \text{ cm}^{-3}$ is the atomic density, v_l , the longitudinal speed of sound, and v_t , the transverse speed of sound. We measured v_l of our sample by picosecond acoustics and found $v_l = 3.35 \text{ km s}^{-1}$. Unpublished computational studies suggest $v_t/v_l \approx 0.70$ in the c direction.¹⁹ Therefore, $\Lambda_{\min} = 0.71 \text{ W m}^{-1} \text{ K}^{-1}$.

Data for several other oxide materials are included in Fig. 3 for comparison. The thermal conductivity of the perovskite PbTiO_3 (Ref. 20) increases with decreasing temperature as expected for a dielectric crystal. Muscovite mica²¹ has one of the lowest thermal conductivities of any oxide material near room temperature but still shows a strong temperature dependence at $T < 200$ K; the cause of the low thermal conductivity in the cross-plane direction of mica is most likely due to a combination of exceptionally strong anharmonicity, significant anisotropy of elastic constants, and low speed of sound in the cross-plane direction.²² Clarke and co-workers²³ recently discovered unusually low thermal conductivity along the c -axis direction of the Aurivillius phase $\text{Bi}_4\text{Ti}_3\text{O}_{12}$ through measurements of textured polycrystalline samples.

The low glasslike thermal conductivity suggests that $\text{CsBiNb}_2\text{O}_7$ harbors some type of disorder that strongly dis-

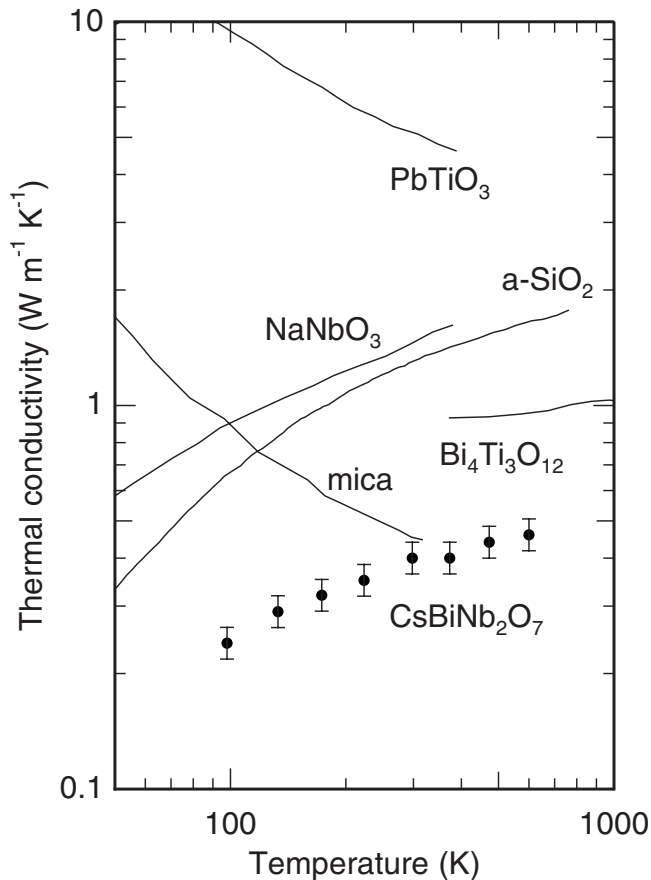


FIG. 3. Temperature dependence of the thermal conductivity (solid circles) of $\text{CsBiNb}_2\text{O}_7$. Error bars indicate an estimated uncertainty of $\pm 10\%$. Data for a variety of oxides are included for comparison. Data for PbTiO_3 and NaNbO_3 are from Ref. 20; data for mica, $\text{Bi}_4\text{Ti}_3\text{O}_{12}$, and amorphous SiO_2 are from Refs. 21, 23, and 28, respectively.

rupts the coherence of acoustic phonons. Similar glasslike conductivity is well-known in relaxor ferroelectrics^{24,25} and even relatively simple oxide compositions such as NaNbO_3 can show low, glasslike thermal conductivity²⁰ although the nature of the disorder in NaNbO_3 , as in $\text{CsBiNb}_2\text{O}_7$, is essentially unknown. We do not believe that clusters of point defects created by the deposition process^{26,27} alone could produce glasslike thermal conductivity. High densities of defects in crystals¹ can have this effect but the density that is required is typically very high; for example, in fluorite-structure crystals of $\text{Ba}_{1-x}\text{La}_x\text{F}_{2+x}$, glasslike thermal conductivity is observed only at $x > 0.1$.

In conclusion, we have identified low thermal conductivity in a layered oxide crystal, $\text{CsBiNb}_2\text{O}_7$, in the Dion–Jacobson family of crystal structures. The conductivity near

room temperature is among the lowest values ever observed in a fully-dense, equilibrium phase of an oxide.

This research was supported by DARPA and the U.S. Department of Energy Grant No. DE-FG02-07ER46459. Experiments were carried out in the Laser and Spectroscopy Laboratory of the Materials Research Laboratory at the University of Illinois, which is partially supported by the U.S. Department of Energy under Grant No. DE-FG02-07ER46453. We thank A. Chernatynskiy and S. Phillpot for sharing their results with us prior to publication.

- ¹D. G. Cahill, S. K. Watson, and R. O. Pohl, *Phys. Rev. B* **46**, 6131 (1992).
- ²R. M. Costescu, M. A. Wall, and D. G. Cahill, *Phys. Rev. B* **67**, 054302 (2003).
- ³C. Chiriac, D. G. Cahill, N. Nguyen, D. Johnson, A. Bodapati, P. Keblinski, and P. Zschack, *Science* **315**, 351 (2007).
- ⁴A. Chernatynskiy, R. W. Grimes, M. A. Zurbuchen, D. R. Clarke, and S. R. Phillpot, *Appl. Phys. Lett.* **95**, 161906 (2009).
- ⁵A. Snedden, K. S. Knight, and P. Lightfoot, *J. Solid State Chem.* **173**, 309 (2003).
- ⁶C. J. Fennie and K. M. Rabe, *Appl. Phys. Lett.* **88**, 262902 (2006).
- ⁷R. J. Goff, D. Keeble, P. A. Thomas, C. Ritter, F. D. Morrison, and P. Lightfoot, *Chem. Mater.* **21**, 1296 (2009).
- ⁸J. C. Clark, J. P. Maria, K. J. Hubbard, and D. G. Schlom, *Rev. Sci. Instrum.* **68**, 2538 (1997).
- ⁹J. B. Nelson and D. P. Riley, *Proc. Phys. Soc. London* **57**, 160 (1945).
- ¹⁰J. L. Hutchison, J. S. Anderson, and C. N. R. Rao, *Proc. R. Soc. London, Ser. A* **355**, 301 (1977).
- ¹¹M. A. Zurbuchen, W. Tian, X. Pan, D. Fong, S. Streiffer, M. E. Hawley, J. Lettieri, Y. Jia, G. Asayama, S. J. Fulk, D. J. Comstock, S. Knapp, A. Carim, and D. G. Schlom, *J. Mater. Res.* **22**, 1439 (2007).
- ¹²Y. K. Koh, S. L. Singer, W. Kim, J. M. O. Zide, H. Lu, D. G. Cahill, A. Majumdar, and A. C. Gossard, *J. Appl. Phys.* **105**, 054303 (2009).
- ¹³H.-K. Lyee and D. G. Cahill, *Phys. Rev. B* **73**, 144301 (2006).
- ¹⁴X. Zheng, D. G. Cahill, and J.-C. Zhao, *Adv. Eng. Mater.* **7**, 622 (2005).
- ¹⁵D. G. Cahill, *Rev. Sci. Instrum.* **75**, 5119 (2004).
- ¹⁶M. Tachibana, H. Kawaji, and T. Atake, *Phys. Rev. B* **70**, 064103 (2004).
- ¹⁷W. Schnelle, R. Fischer, and E. Gmelin, *J. Phys. D: Appl. Phys.* **34**, 846 (2001).
- ¹⁸K. S. Gavrichev, V. E. Gorbunov, L. N. Golushina, G. A. Totorova, E. A. Tishchenko, Y. G. Nadtochi, and Y. B. Poyarkov, *Inorg. Mater.* **30**, 1346 (1994).
- ¹⁹A. Chernatynskiy and S. Phillpot, “Tba,” Private communication.
- ²⁰M. Tachibana, T. Kolodiazny, and E. Takayama-Muromachi, *Appl. Phys. Lett.* **93**, 092902 (2008).
- ²¹A. S. Gray and C. Uher, *J. Mater. Sci.* **12**, 959 (1977).
- ²²W.-P. Hsieh, B. Chen, J. Li, P. Keblinski, and D. G. Cahill, *Phys. Rev. B* **80**, 180302(R) (2009).
- ²³Y. Shen, D. R. Clarke, and P. A. Fuierer, *Appl. Phys. Lett.* **93**, 102907 (2008).
- ²⁴J. J. De Yoreo, R. O. Pohl, and G. Burns, *Phys. Rev. B* **32**, 5780 (1985).
- ²⁵M. Tachibana, K. Sasame, H. Kawaji, T. Atake, and E. Takayama-Muromachi, *Phys. Rev. B* **80**, 094115 (2009).
- ²⁶T. Ohnishi, K. Shibuya, T. Yamamoto, and M. Lippmaa, *J. Appl. Phys.* **103**, 103703 (2008).
- ²⁷D. A. Freedman, D. Roundy, and T. A. Arias, *Phys. Rev. B* **80**, 064108 (2009).
- ²⁸D. G. Cahill, *Rev. Sci. Instrum.* **61**, 802 (1990).